Journal of Achievements in Materials and Manufacturing Engineering
VOLUME 49
ISSUE 2
December
2011

Theoretical basis of Al-Si coat crystallization on gray and nodular cast iron and making the layered items using it

S. Pietrowski*, T. Szymczak
Department of Materials Engineering and Production Systems,
Technical University of Łódź, ul. Stefanowskiego 1/15, 90-924 Łódź, Poland
* Corresponding author: E-mail address: tomasz.szymczak@p.lodz.pl

Received 12.10.2011; published in revised form 01.12.2011

Manufacturing and processing

ABSTRACT

Purpose: The aim of this study was to present studies of crystallization and the construction of the coat consisting of Al-Si alloys, also with alloy additives: Ni, Cu and Mg, deposited on gray and nodular cast iron, and the connection through this coat the layered item. On this basis, a model of creating a coat and layered item was developed.
Design/methodology/approach: Studies of coats and layered products were carried out on scanning electron and optical microscopes. The chemical microanalysis and diffraction of backward scattered atoms in the characteristic areas of the coat and substrate material was made.
Findings: : In this paper the influence of the most important technological factors on the thickness and phase construction of the silumin coat and connection quality in the layered item was presented.
Research limitations/implications: Currently, research of dip application of coats made of silumins containing: Cu, Ni, Mg, Cr, Mo, W and V on non-alloy and alloy steels and the manufacture of layered items to their use are conducted.
Practical implications: Dip coats are used as protective coats or intermediate coat of layered item. The paper presents an example of the implementation for the manufacture of the layered items low-alloyed gray cast iron-silumin coat-silumin reciprocating compressor body for room air conditioning.
Originality/value: Originality of the paper consists in elaborating of the theoretical model of forming the diffusion layer made of Al-Si-M silumin on iron alloys. Theoretical basis of layers production were elaborated too. They are significant for collar fillings production in high-pressure combustion engines pistons, as anticorrosive layers and for layered items production.
Keywords: Casting; Nodular and gray cast iron; Al-Si coat; Layered item

Reference to this paper should be given in the following way:
S. Pietrowski, T. Szymczak, Theoretical basis of Al-Si coat crystallization on gray and nodular cast iron and making the layered items using it, Journal of Achievements in Materials and Manufacturing Engineering 49/2 (2011) 421-439.

1. Introduction

The process of dipping application of the coat made of Al-Si alloys, probably with alloy additives: Ni, Mg and Cu, on ferrous alloys is generally called alphinating. However, the name "silumin coats" is more correct because it reflects the idea of the process. This process was used for the first time to obtain joining of the collar filling with the cylinder made of silumins. This process is used nowadays for cylinders of powerful combustion engines with auto-ignition [1].

Another example of Al-Si coat use is production of the layered cast of the suspension bush of a car made of silumin AS7G (6.9% Si, 0.3% Mg, 0.04% Mn, 0.15% Fe) with a nodular cast iron insert, which is presented in this work [2].

It also describes the structure of the joining. The joining area has a small thickness of about 12 μm, thus it is not possible to generalize its structure and relate to the coats with bigger thickness. It was stated that from the cast iron side there is a thin layer of the phase Al_5Fe_2, the following layers are phases $Al_{7,4}Fe_2Si$ and $Al_{4,4}Fe_2Si$ and the components of silumin α(Al) and eutectics (α+β) (Al+Si). This structure was not proved in the works [3,4]. Another example is the use of Al-Si coats on steel and cast iron as anticorrosive coatings, for instance, on some elements of the car body, perforated pipes, telecom wires, nets and steel strapping [3,5]. Silicon in the coat gives it plasticity because it protects against penetration of crystallites of the phase Al_5Fe_2 into the base [6]. The data presented from the scientific literature does not provide any theoretical basis of the coat crystallization and its special structure.

Nowadays the industry aims at obtaining cheap and light items, which makes it possible to use the presented Al-Si coats more widely, first of all to produce layered items of the type ferrous alloys - Al-Si alloys as well with alloy additives which are often used in silumins, i.e. Ni, Cu and Mg. That is why the Department of Material Technology and Productive Systems of the Łódź University of Technology started researching crystallization of Al-Si coats, their phase structure and layered items which are used in them. Some research results were published in works [3,7-12].

They refer to the Al-Si coat application on non-alloyed and alloyed steels as well as on gray and nodular cast iron. The current work presents further research on syntheses of the theoretical basis of Al-Si coats crystallization and producing layered elements from gray and nodular cast iron in connection with silumins.

2. Results and analysis

The thickness and the coat structure from Al-Si alloys applied on ferrous alloys (steel, cast-steel and cast iron) depend on the following factors:

- the kind of the dipped material and its microstructure,
- the shape, section, roughness height and temperature of the dipped element,
- the chemical composition of Al-Si alloy, and especially the concentration of silicon in it.
- the temperature of the bath,
- the holding time of the ferrous alloy in the Al-Si bath.

The coat applied on ferrous alloys as a rule consists of three layers and their structure depends on the kind of the ferrous alloy. Before application of the coat the object has to be thoroughly cleaned and degreased and preliminary heated at the temperature not more than 150°C so that ferrous oxides would not form on it. Then the object is dipped into the bath. Regarding the significant temperature difference between the object and the bath it is possible that the layer of Al-Si alloy crystallizes on it, which melts as the temperature of the object grows. The temperature of the bath around the object decreases. The process of crystallization of the coat starts when the object reaches the so called temperature of the contact "t_s". It is the temperature which appears on the surface of the two ideally contacting bodies. At that time the homogeneity of the temperature and the stream of heat on the contact surface occur [13]. The temperature "t_s" is described by the following dependence:

$$t_s = \frac{\sqrt{\lambda_k \cdot c_k \cdot \rho_k} \cdot t_k + \sqrt{\lambda_{Fe} \cdot c_{Fe} \cdot \rho_{Fe}} \cdot t_{Fe}}{\sqrt{\lambda_k \cdot c_k \cdot \rho_k} + \sqrt{\lambda_{Fe} \cdot c_{Fe} \cdot \rho_{Fe}}} \tag{1}$$

where:
λ_k, λ_{Fe} - the coefficient of thermal conductivity of the Al-Si bath and the ferrous alloy element correspondently, W/m·K
c_k, c_{Fe} - the specific heat of the bath and the ferrous alloy element, J/kg·K,
ρ_k, ρ_{Fe} - the specific mass of the bath and the ferrous alloy element, kg/m^3,
t_k - the temperature of the bath, °C,
t_{Fe} - the temperature of the ferrous alloy element at the moment of dipping, °C.

Beginning with the temperature „t_s", heating of the surface layer of the object and the neighbouring liquid bath Al-Si take place. Figure 1 (a-d) exemplifies the results of the simulation of the time needed to obtain the temperature "t_s" in the AlSi11 bath for the rod with the radius of r = 5 mm and the height of h = 50 mm made of gray cast iron EN-GJL-250. The simulation was made using the FlexPDE 5.0.9 computer application.

It shows that the contact temperature "t_s" was obtained 2.1 s after the moment the specimen was dipped into the liquid AlSi11 bath. For the same specimen made of, let us say, "armco" iron the temperature "t_s" was achieved in 2.5 s. The relatively small difference in the time was caused, first of all, by the density of both alloys ("armco" - ρ = 7870 kG/m^3, cast iron - ρ = 7300 kG/m^3) and the presence of temper graphite which increases thermal conductivity of cast iron.

The increase in the temperature of the Al-Si bath as a result of minimizing the reach of the temperature "t_s" increases the thickness of the coat on steel and the cast iron, which is exemplified in Figure 2 for cast iron EN-GJL-250 dipped in the AlSi11 bath.

It shows that at the bath temperature t_k = 650°C the thickness of the coat is not big (~55 μm), it is not continuous and irregular. The thickest coat (~260 μm) was obtained at the bath temperature t_k = 950°C. However, at this temperature results in fragmentation of the coat and it is very hermetic. This phenomenon takes place at temperatures above t_k = 800°C. The dipping time of the object in the Al-Si bath has the same influence on the coat construction. The carried out research showed that the optimal coat is obtained at the bath temperature t_k = 750°C for the holding temperature τ = 180 s, which is shown in Figure 3 (a, b).

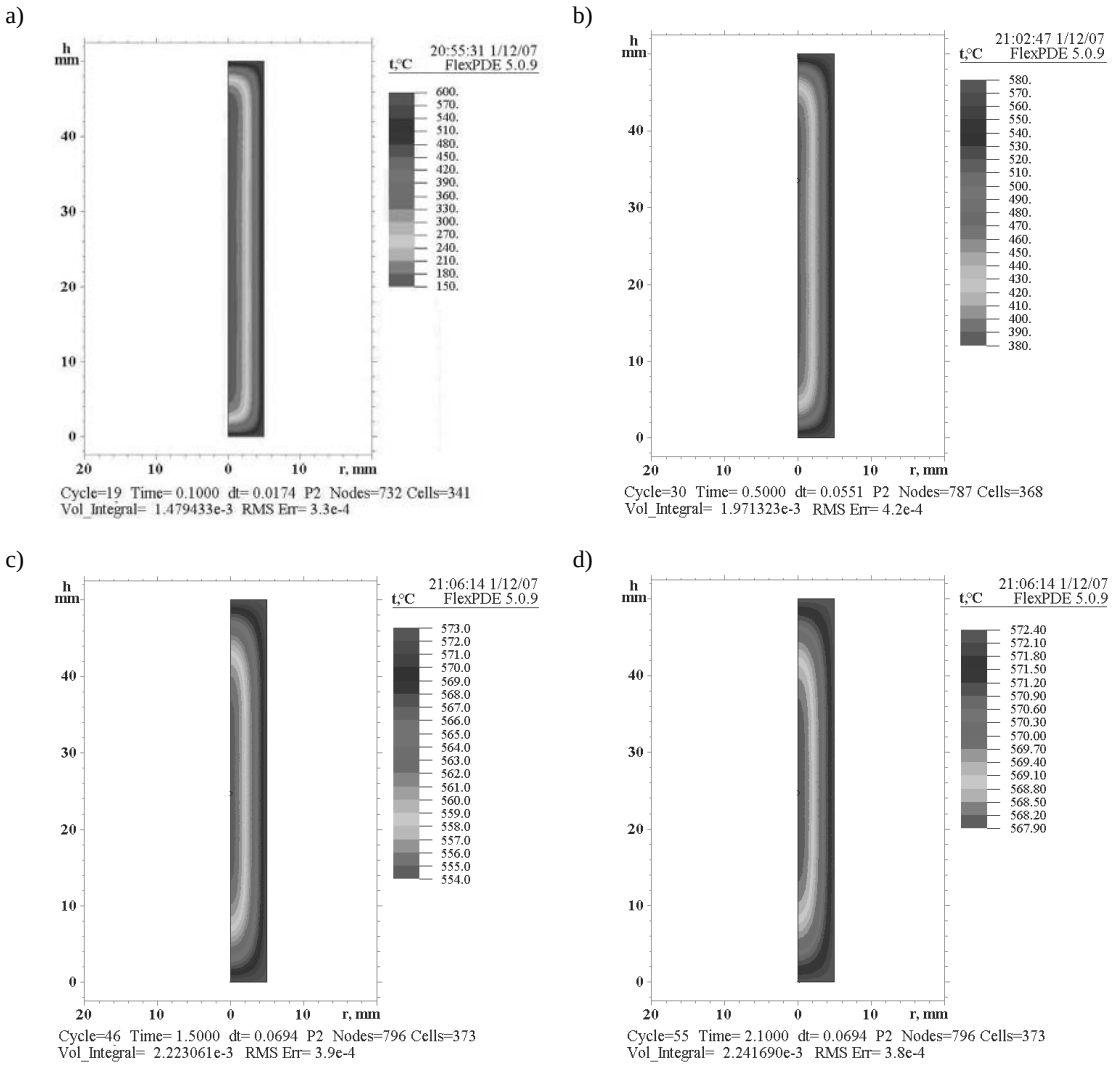

Fig. 1. The simulation results of the temperature „t_s" obtained in: a) 0.1 s; b) 0.5 s; c) 1.5 s; d) 2.1 s

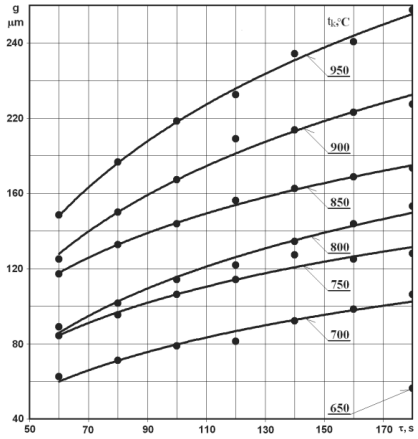

Fig. 2. The influence of the bath temperature "t_k" and the holding time "τ" on the coat thickness on gray cast iron

a)

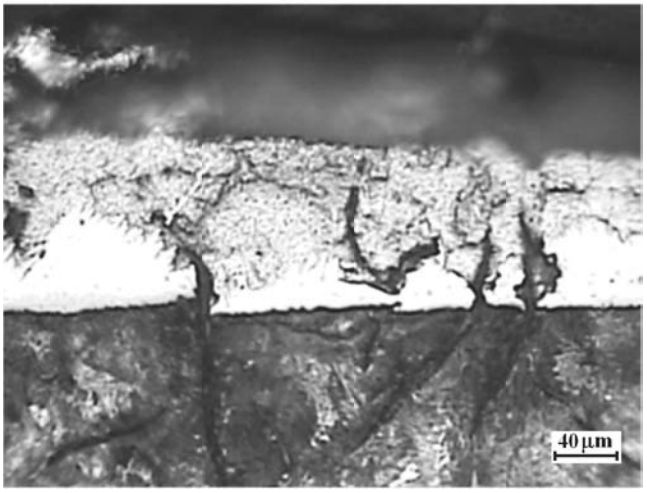

b)

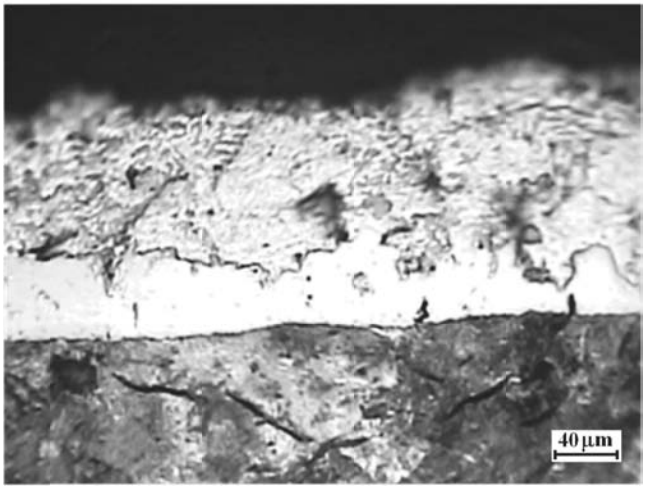

Fig. 3. The coat alphinated in the bath at t_k = 750°C and for the time: a) 60 s, b) 180 s

It shows that the coat consists of two layers, the first one marked as "g_1" which joins the object immediately and the second one "g_2" which joins the "g_1" layer. The total thickness of the coat which is "g_1 + g_2" was marked as "g". Figure 4 shows the influence of the silicon concentration in the bath on the thickness of the layer "g_1" and the coat "g".

It shows that the increase in the Si concentration in the bath decreases the thickness of the layer "g_1" and the whole coat "g". The influence of the silicon concentration in the bath on the thickness and the construction of the coat in gray cast iron is shown in Figure 5 (a-f).

It follows from Fig. 5 (a-f) that the increase in the silicon concentration changes the structure and the thickness of the layer "g_1". The layers obtained in pure aluminum and in AlSi1.5 alloy (Fig. 5 a, b) are characterized by a close column structure. The further increase in the Si concentration changes the column structure of the layer into a faced structure (Fig. 5 c-f) and causes a slight non-continuity of the layer at 12.0 and 17.0% of Si. In order to describe the kind of phases appearing in the coat made of aluminum and AlSi1.5 alloy on gray cast iron, the point-counter analysis of the elements concentration in the diffusive layer "g_1" was carried out. Three elements appeared there: iron, aluminum and silicon for AlSi1.5; their average concentrations are presented in Table 1.

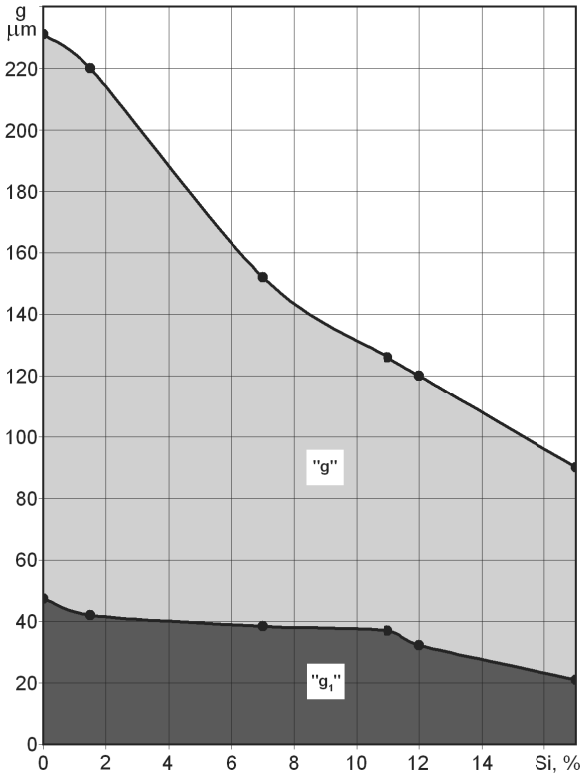

Fig. 4. The influence of Si concentration in the bath on the thickness of the layer "g_1" and "g"

Table 1.
The average concentration of Al, Fe and Si (for alloy AlSi1.5) in the layer "g_1"

Element	k-ratio (calc.)	ZAF	Atom %	Element Wt %	Wt % Err. (1-Sigma)
Al-K	0.3580	1.467	68.85	52.52	+/- 0.25
Si-K	0.0093	1.852	2.16	1.72	+/- 0.10
Fe-K	0.4203	1.089	28.99	45.77	+/- 0.59
Total			100.00	100.00	

It shows that the layer "g_1" obtained in the aluminum bath is made of the Al_3Fe phase. The increase in the Si concentration in the bath would cause the appearance of phases of $Al_{12}Fe_3Si_2$ and $Al_9Fe_3Si_2$ in the layer "g_1", and of the silumin components in the layer "g_2", i.e. α and α+β eutectics, as exemplified in Figure 6 (a, b) and in Tables 2-5.

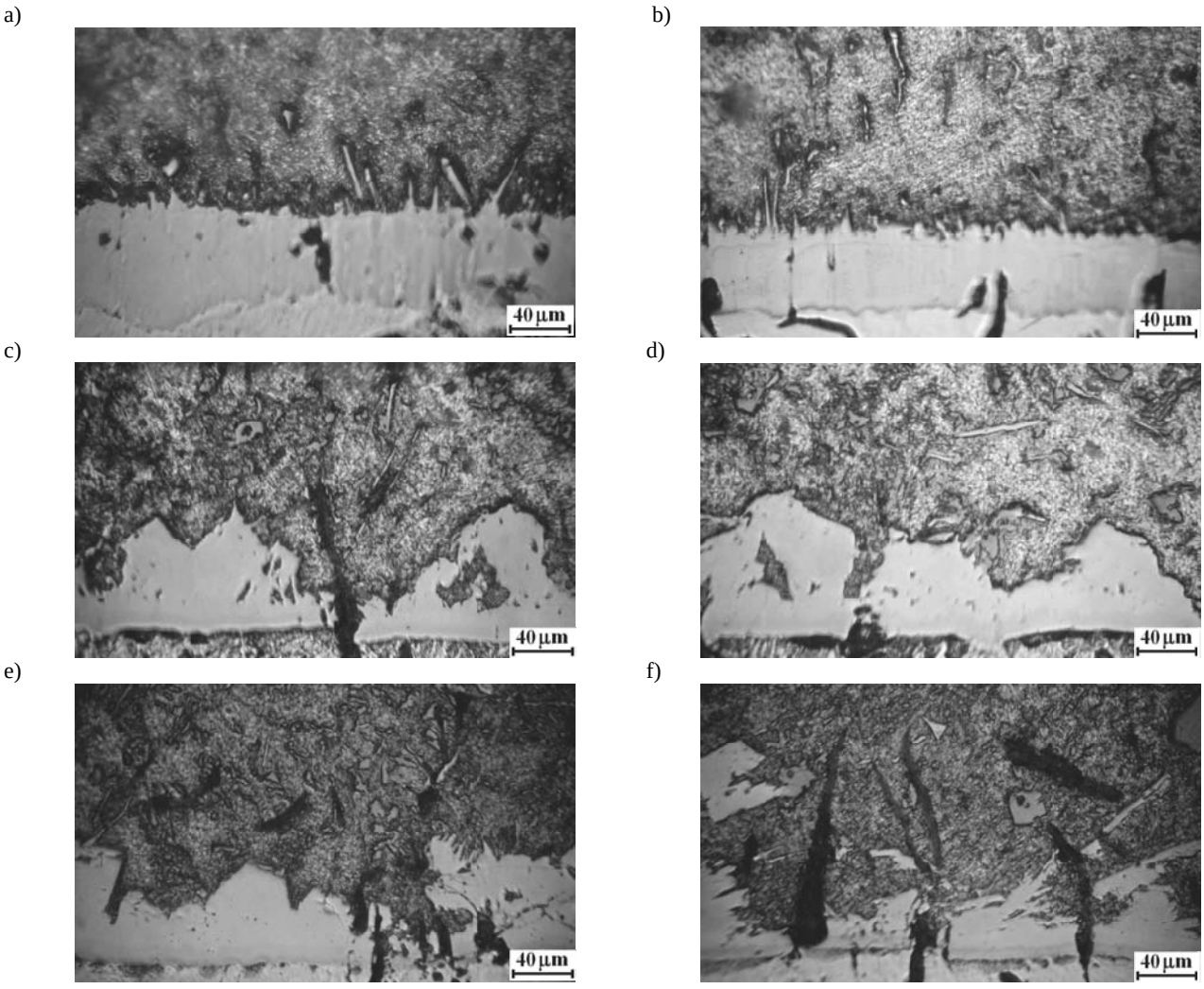

Fig. 5. The influence of Si concentration in the bath on the thickness and the construction of the coat on gray cast iron: a) 0.0% Si, b) 1.5% Si, c) 7.0% Si, d) 11.0% Si, e) 12.0% Si, f) 17.0% Si

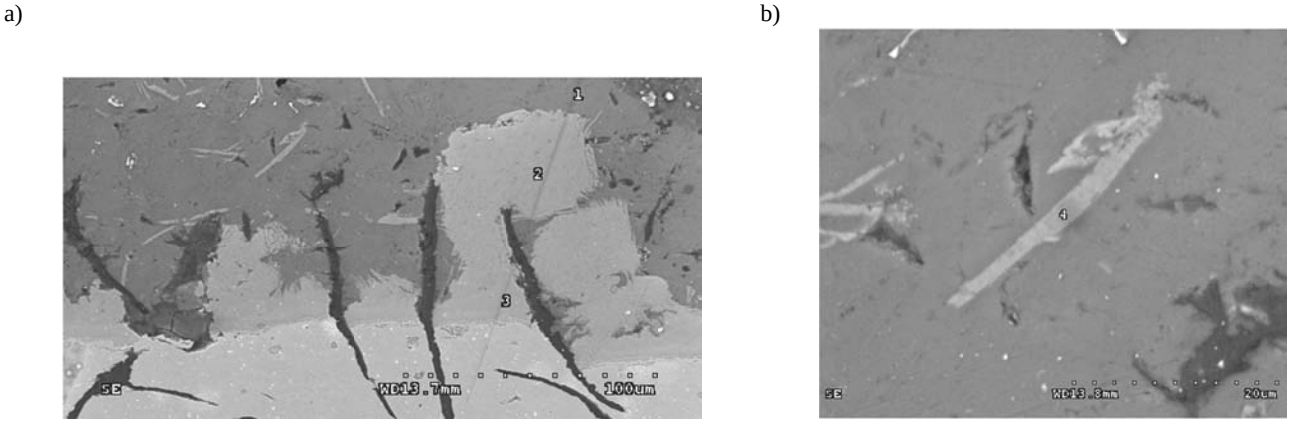

Fig. 6. Measuring points of concentration: Al, Fe and Si in the coat on gray cast iron obtained in the bath AlSi11 of t_k = 750°C and within the time of τ = 180 s

Table 2.
Concentration: Al, Fe and Si in measuring point "1"

Element	k-ratio (calc.)	ZAF	Atom %	Element Wt %	Wt % Err. (1-Sigma)
Al-K	0.9727	1.008	98.39	98.02	+/- 0.45
Si-K	0.0059	2.283	1.30	1.35	+/- 0.11
Fe-K	0.0054	1.165	0.31	0.63	+/- 0.22
	Total		100.00	100.00	

Table 3.
Concentration: Al, Fe and Si in measuring point "2"

Element	k-ratio (calc.)	ZAF	Atom %	Element Wt %	Wt % Err. (1-Sigma)
Al-K	0.3980	1.387	67.74	55.19	+/- 0.27
Si-K	0.0515	1.888	11.46	9.72	+/- 0.11
Fe-K	0.3162	1.110	20.81	35.09	+/- 0.61
Total			100.00	100.00	

Table 4.
Concentration: Al, Fe and Si in measuring point "3"

Element	k-ratio (calc.)	ZAF	Atom %	Element Wt %	Wt% Err. (1-Sigma)
Al-K	0.3534	1.471	66.90	51.98	+/- 0.25
Si-K	0.0279	1.894	6.53	5.28	+/- 0.08
Fe-K	0.3902	1.095	26.58	42.74	+/- 0.59
Total			100.00	100.00	

Table 5.
Concentration: Al, Fe and Si in measuring point "4"

Element	k-ratio (calc.)	ZAF	Atom %	Element Wt %	Wt % Err. (1-Sigma)
Al-K	0.4683	1.284	69.87	60.15	+/- 0.30
Si-K	0.0741	1.891	15.64	14.01	+/- 0.21
Fe-K	0.2294	1.126	14.50	25.84	+/- 0.58
Total			100.00	100.00	

Table 6.
Concentration: Al, Fe and Si in measuring point "1"

Element	k-ratio (calc.)	ZAF	Atom %	Element Wt %	Wt % Err. (1-Sigma)
Al-K	0.9764	1.007	98.62	98.27	+/- 0.46
Si-K	0.0053	2.143	1.09	1.13	+/- 0.17
Fe-K	0.0051	1.164	0.29	0.60	+/- 0.22
Total			100.00	100.00	

Table7.
Concentration: Al, Fe and Si in measuring point "2"

Element	k-ratio (calc.)	ZAF	Atom %	Element Wt %	Wt % Err. (1-Sigma)
Al-K	0.4002	1.352	66.73	54.09	+/- 0.27
Si-K	0.0565	1.777	11.92	10.07	+/- 0.17
Fe-K	0.3232	1.108	21.35	35.84	+/- 0.63
Total			100.00	100.00	

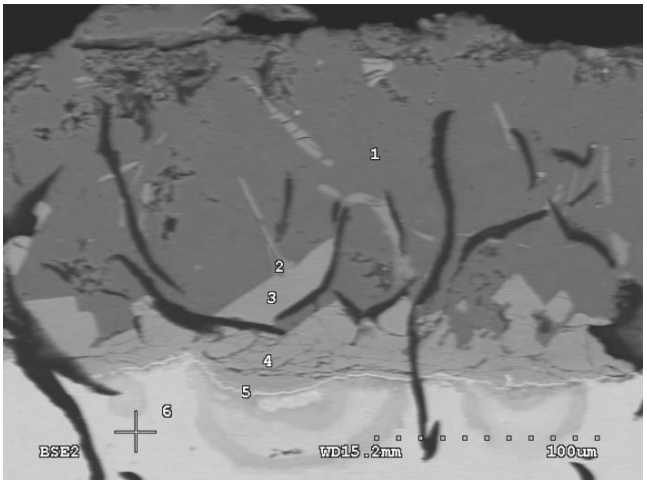

Fig. 7. The area of the specimen from gray cast iron with the coat applied in silumin AlSi11 at t_k = 750°C and for the time τ = 180 s with the marked points of diffraction 1-6

It follows from the presented data that in point "1" in the area of the layer "g_2" phase "α" (Al) and a minimal quantity of Si = 1.35% appears (Tab. 2). In point "2", 55.19% Al, 35.0% Fe and 9.72% Si appear (Tab. 3). It is the phase which is close to $Al_{12}Fe_3Si$. In point "3" there was an increase in Al to 51.98% and Fe to 42.74% and a decrease in Si to 5.28% (Tab. 4). In the phase with point "4", appearance of 60.15% Al, 25.84% Fe and 14.01% Si (Tab. 5) was noted. This phase is close to the phase $Al_9Fe_3Si_2$ which in the balanced state includes: 59.05% Al, 27.17% Fe and 13.77% Si [14,15]. In order to determine the precise phase structure of the certain layers of the coat on cast iron, which is very similar to the coats made on steels, which is shown in the further part of the work, the tested gray cast iron was subdued to electron diffraction previously diffused in the area of these layers. The results of the diffraction concerned the coat applied in silumin AlSi11 at t_k = 750°C and for the time τ = 180 s. The area of the specimen with the applied coat and marked points of diffraction 1-6 is shown in Figure 7.

Examples of diffraction patterns and phases identification are presented in Figure 8-11 (a-c).

The similar thickness and structure of the coat in the function of the factors presented for gray cast iron EN-GJL-250 is obtained in nodular cast iron EN-GJS-500-7.

The coats on nodular cast iron are a bit thicker than on gray cast iron. Figure 12 (a, b) exemplified the thickness of the coat on nodular cast iron obtained in silumin AlSi11 at t_k = 750°C and for the time τ = 120 s and 180 s respectively.

Nodular graphite precipitations are also seen in the coat. The presented example of the test area of the elements concentration in the coat on nodular cast iron is shown in Fig. 13.

Typical in this case is appearance of the third layer in the coat which directly adjoins cast iron marked as No "3". This layer did not appear in gray cast iron. Tables 6-9 show the concentration of the tested elements in measuring points "1-4".

a)

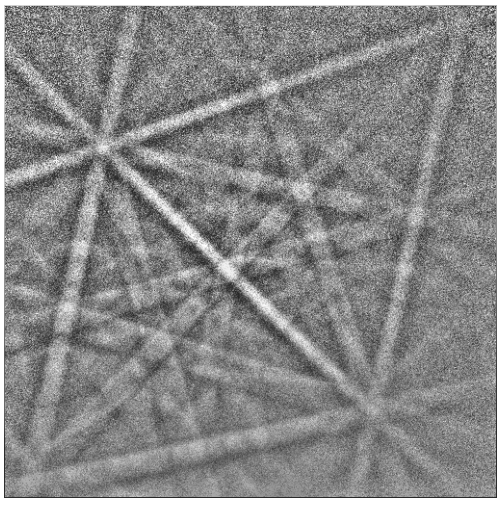

b)

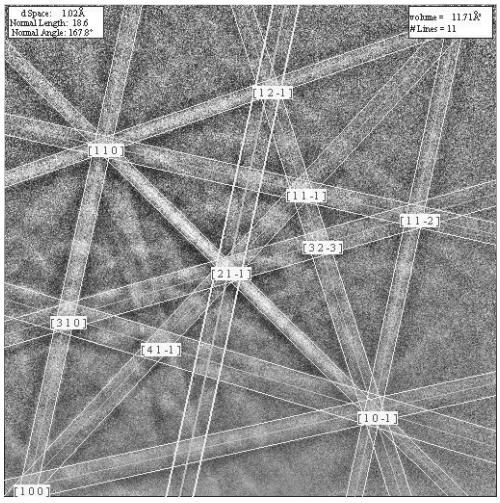

c)

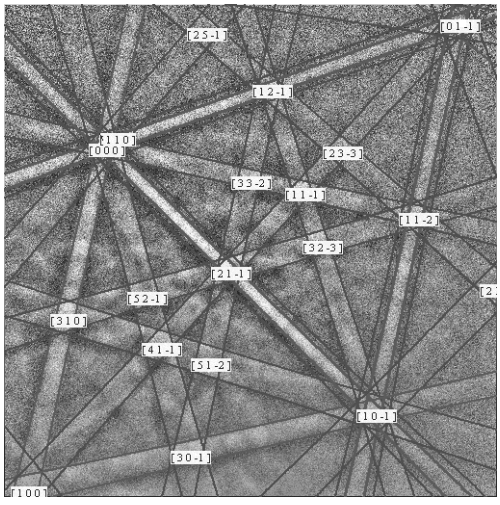

Fig. 8 (a-c). A diffractive picture of area 1 from Fig. 7 (a); an indicated picture of micro-area No 1 (b) and the simulation of the picture for aluminum (c)

a)

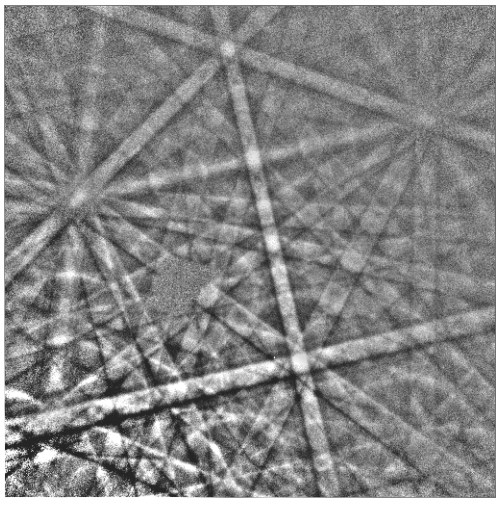

b)

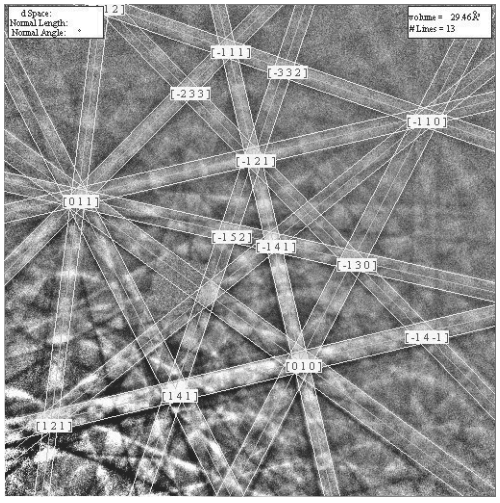

c)

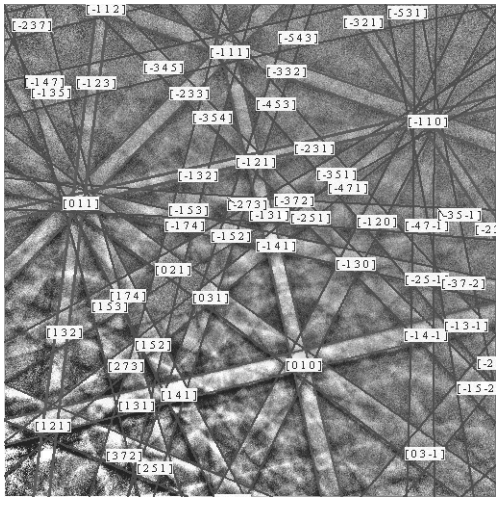

Fig. 9 (a-c). A diffractive picture of micro-area No 2 from Fig. 7 (a); an indicated picture of micro-area No 2 (b) and the simulation of the picture for silicon (c)

a)

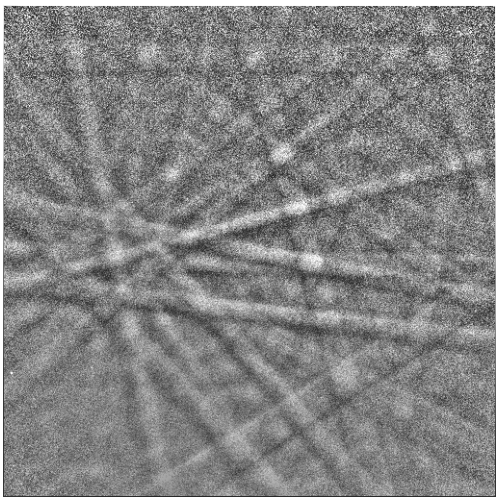

b)

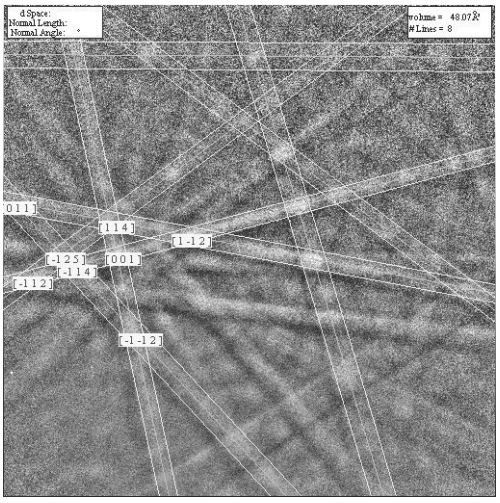

c)

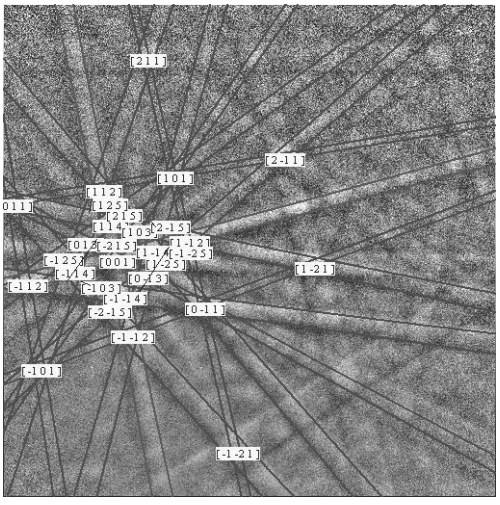

Fig. 10 (a-c). A diffractive picture of phase No 3 from Fig. 7 (a); an indicated picture of phase No 3 (b) and the simulation of the picture for $Al_9Fe_3Si_2$ (c)

a)

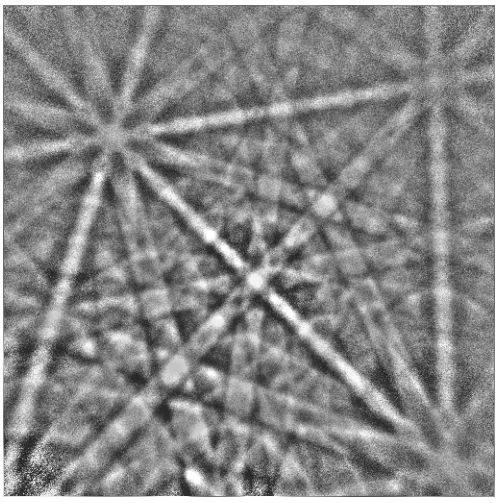

b)

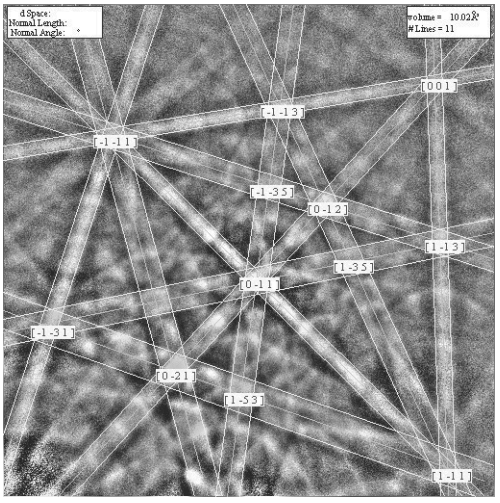

c)

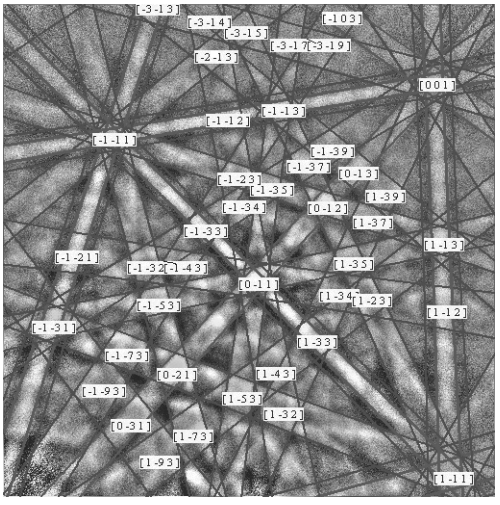

Fig. 11 (a-c). A diffractive picture of micro-area No 6 from Fig. 7 (a); an indicated picture of micro-area No 6 (b) and simulation of the picture for the ferrite (c)

a)

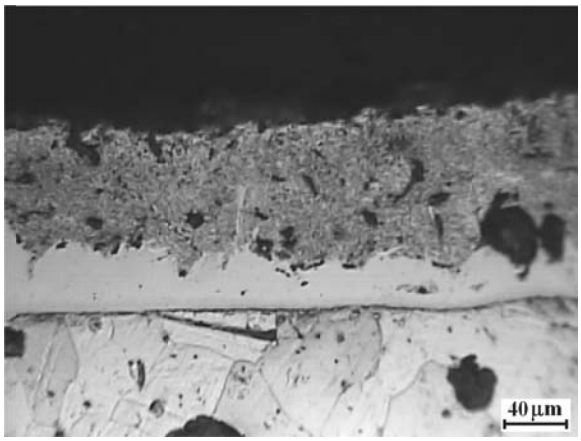

b)

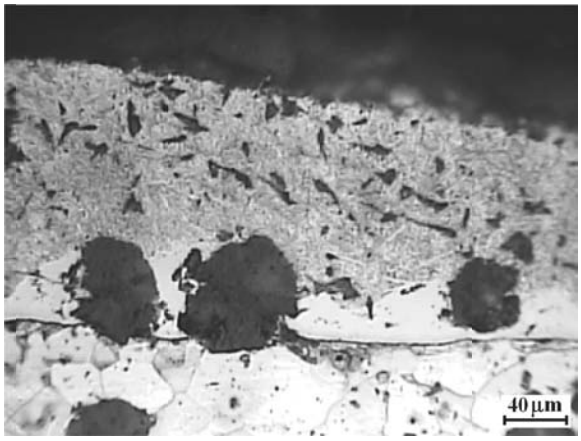

Fig. 12 (a, b). The example of the coat on nodular cast iron obtained in the bath AlSi11 at t_k = 750°C and for the time τ = 180 s i τ = 180 s respectively.

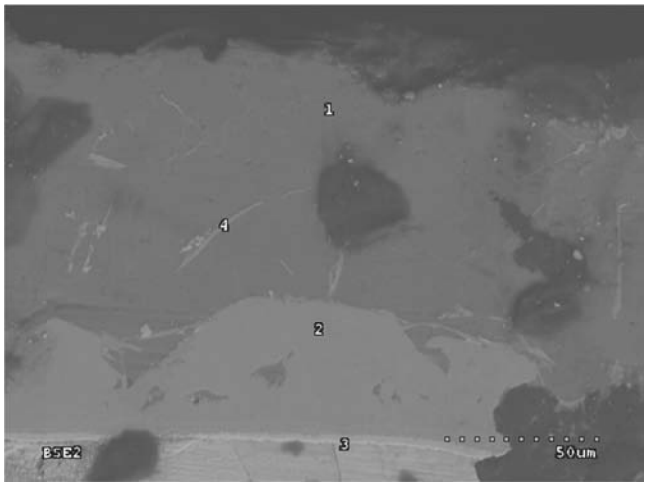

Fig. 13. Measuring points of the concentration test: Al, Fe and Si in the coat on nodular cast iron obtained after the holding time τ = 180 s in silumin AlSi11 at t_k = 750°C

Table 8.
Concentration: Al, Fe and Si in measuring point "3"

Element	k-ratio (calc.)	ZAF	Atom %	Element Wt %	Wt % Err. (1-Sigma)
C -K	0.0141	4.364	21.26	6.14	+/- 0.42
Al-K	0.0040	1.836	1.12	0.73	+/- 0.07
Si-K	0.0780	1.451	16.74	11.31	+/- 0.11
Fe-K	0.7833	1.044	60.88	81.82	+/- 0.67
Total			100.00	100.00	

a)

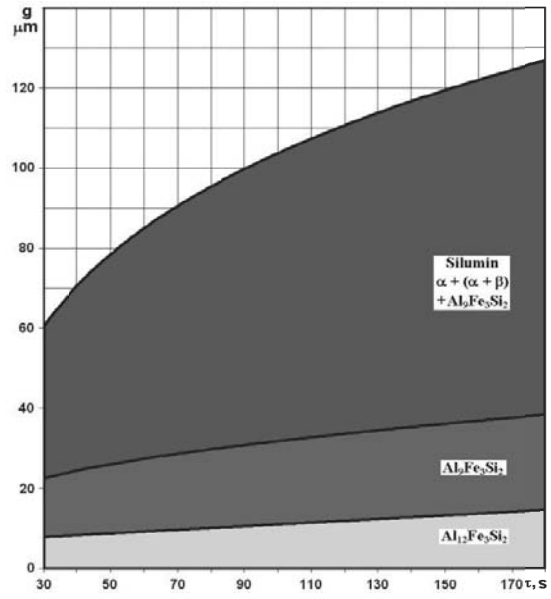

b)

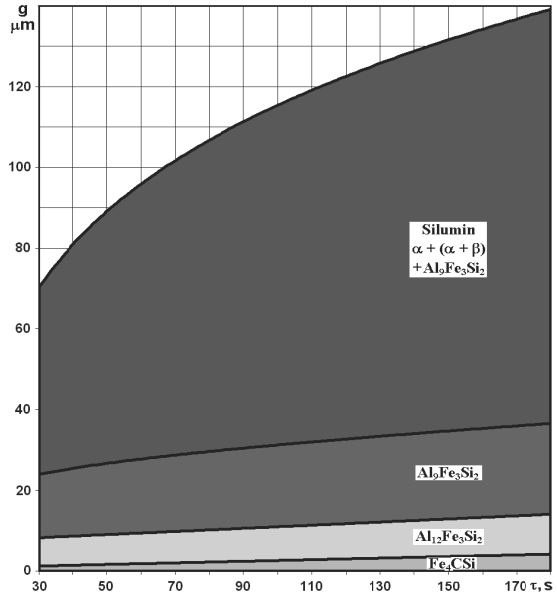

Fig. 14 (a, b). The thickness of the composing layers of the coat on gray cast iron (a) and nodular cast iron (b) in the function of the holding time "τ"

Table 9.
Concentration: Al, Fe and Si in measuring point "4"

Element	k-ratio (calc.)	ZAF	Atom %	Element Wt %	Wt % Err. (1-Sigma)
Al-K	0.4712	1.315	70.85	62.81	+/- 0.26
Si-K	0.1702	1.937	17.36	16.04	+/- 0.25
Fe-K	0.1983	1.123	11.79	21.15	+/- 0.52
Total			100.00	100.00	

It follows from the presented data that in measuring points 1, 2 and 4 phases analogous to those in the coat on gray cast iron appear, i.e. Al, $Al_9Fe_3Si_2$, $Al_{12}Fe_3Si_2$ respectively; however, in point "4" carbide Fe_4CSi appears [16]. It should be supposed that appearance of the layer of carbide Fe_4CSi directly on the ground of nodular cast iron is caused by easier merging of the pearlite, as a result carbon appears in the liquid layer in cast iron forming iron-silicon carbide Fe_4CSi. Figure 14 (a, b) exemplifies the influence of the holding time "τ" in the AlSi11 bath at t_k = 750°C on the thickness of the particular composing layer in the coat.

If shows that on gray cast iron the thickness of the layers consisting of the intermetallic phases $Al_{12}Fe_3Si_2$ and $Al_9Fe_3Si_2$ is bigger than that on nodular cast iron, however, the thickness of the whole coat is bigger on nodular cast iron.

The comparative juxtaposition of the concentration of the tested elements in the measuring points of the coat on gray cast iron and nodular cast iron is presented in Figure 15.

The presented data shows a similar concentration of the elements in the phases $Al_{12}Fe_3Si_2$ and $Al_9Fe_3Si_2$ in gray and nodular cast iron. The time "τ" of holding of the element in the bath significantly influences the growth in the concentration: Fe and Si in the phase $Al_9Fe_3Si_2$ appearing in the layer which consists of silumin, i.e. phases: Al, eutectic (Al + Si) and ferroic $Al_9Fe_3Si_2$. In case of the layers adjacent to the base, i.e. $Al_{12}Fe_3Si_2$ and the next one $Al_9Fe_3Si_2$ the time "τ" does not have an influence on the concentration of Al, Fe and Si in them.

The influence of the degree of roughness "Rz" and the arithmetic average roughness "Ra" in the tested cast irons on the thickness of the coat was obtained using different processing accuracy of turning and finishing. The representing profilograms of the surface of the tested cast iron types after machining are shown in Figure 16 (a-d) for gray cast iron and 17 (a-d) for nodular cast iron.

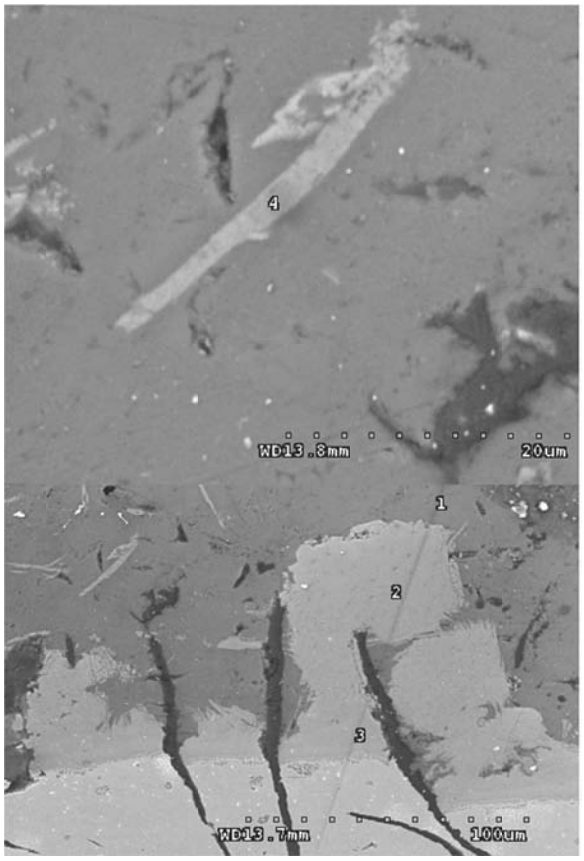

Measuring point No	Element	Concentration of the elements, %		
		Cast iron		
		gray		gray
		Holding time in the bath AlSi11 τ, s		
		120	180	180
1	Al	98.21	98.02	98.27
	Fe	0.39	0.63	0.60
	Si	1.40	1.35	1.13
2	Al	55.33	55.19	54.09
	Fe	35.27	35.09	35.84
	Si	9.40	9.72	10.07
3 (on specimen made of gray cast iron)	Al	41.39	51.98	
	Fe	49.37	42.74	
	Si	9.24	5.28	
3 (on specimen made of nodular cast iron)	Al			0.73
	Fe			81.82
	Si			11.31
	C			6.14
4 (sheet-like phase)	Al	75.69	60.15	62.81
	Fe	14.87	25.84	21.15
	Si	9.43	14.01	16.04

Fig. 15. Comparison of the concentration of the tested elements in the measuring points of the coat on gray and nodular cast iron

a)

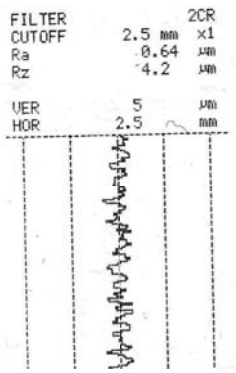

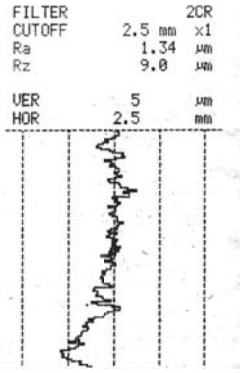

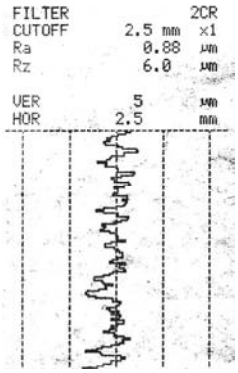

b)

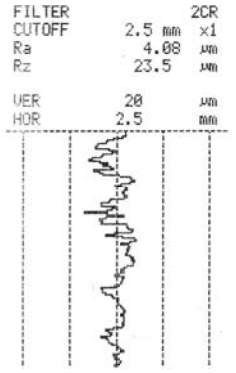

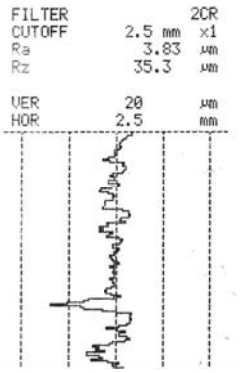

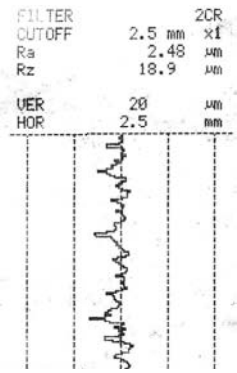

c)

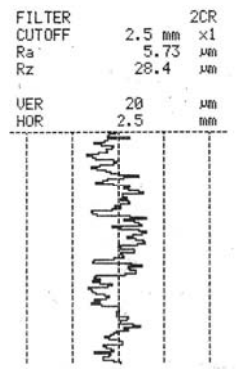

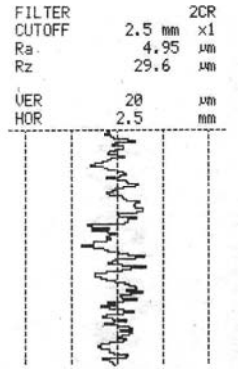

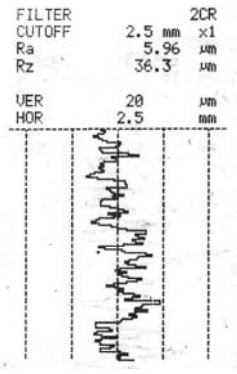

d)

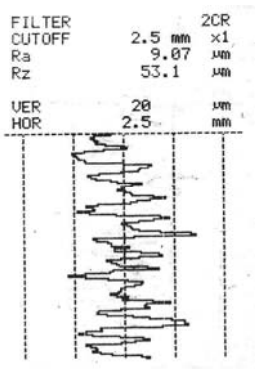

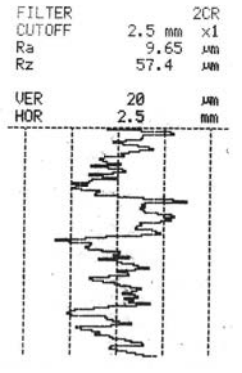

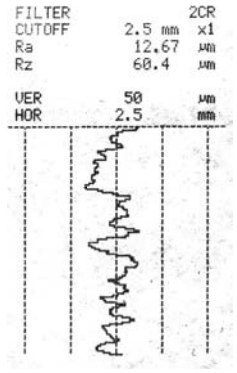

Fig. 16 (a-d) Representative profilograms of the gray cast iron surface after different machining: a - finishing, b - accurate turning 1, c - accurate turning 2, d - rough turning

a)

b)

c)

d)

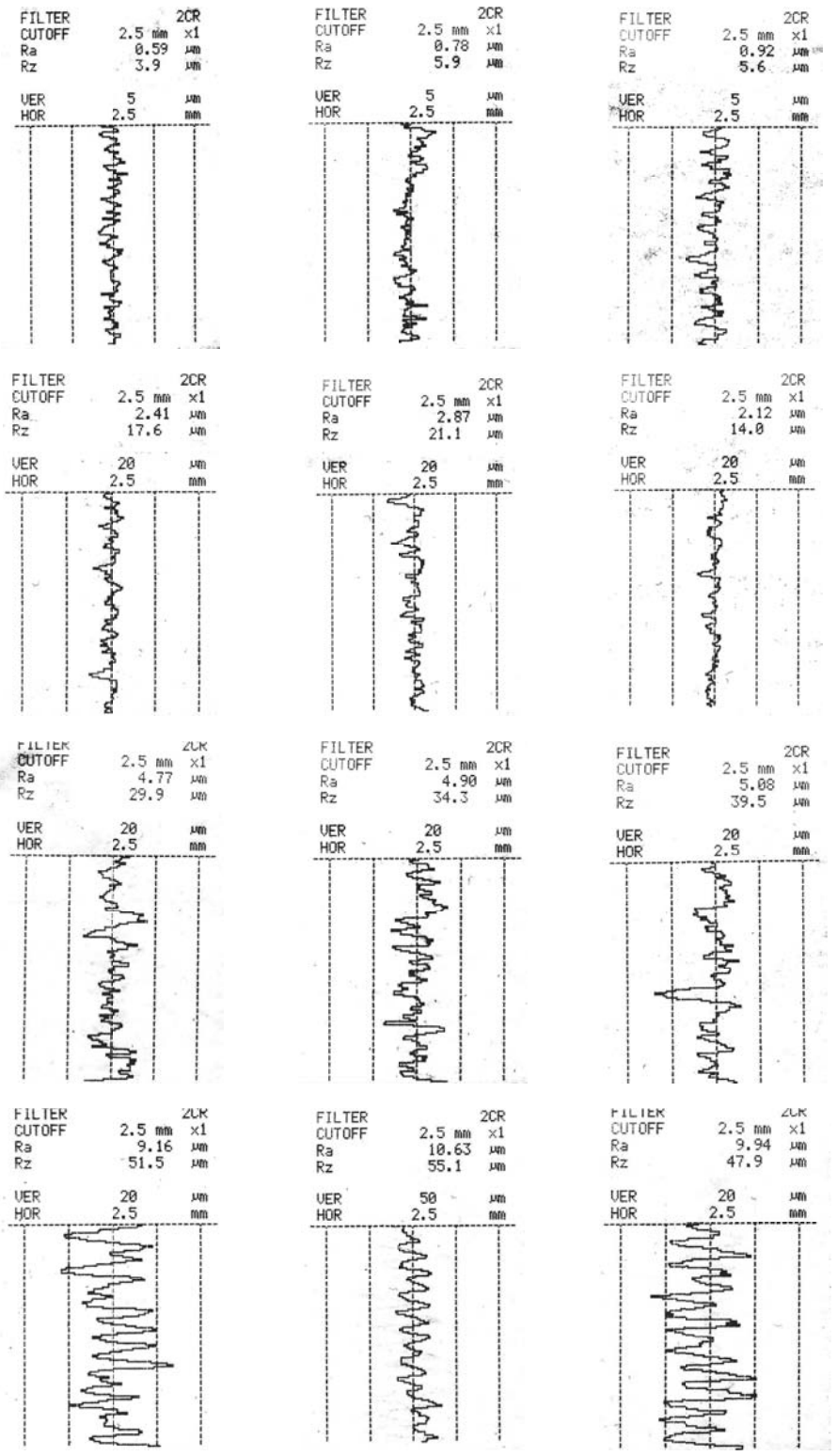

Fig. 17 (a-d). Representative profilograms of the nodular cast iron surface after different machining: a - finishing, b - accurate turning 1, c - accurate turning 2, d - rough turning

The average values of the parameters "Rz" and "Ra" on the tested cast irons after turning and finishing are presented in Table 10.

Table 10.
Average values of the parameters „Rz" and „Ra" obtained on the gray and nodular cast iron after turning and finishing

Kind of machining	Average values of the parameters "Rz" ("Ra"), µm	
	Gray cast iron	Nodular cast iron
Finishing	6.40 (0.95)	5.13 (0.76)
Accurate turning 1	25.90 (3.46)	17.75 (2.47)
Accurate turning 2	31.43 (5.55)	34.57 (4.92)
Rough turning	56.97 (10.46)	51.50 (9.91)

It shows that on nodular cast iron the values of "Rz" and "Ra" are smaller in comparison to gray cast iron. It follows form the data presented in Figures 16 and 17 and in Table 10 that:

- the surface field of the roughness tops is very small in relation to the normal surface field and increases when the surface evenness goes down,
- the slope of the micro-irregularity profile of the processed surfaces with different evenness is bigger when the roughness is bigger,
- the slope of the profile and the curvature of the tops along the processing traces are much smaller than in the direction perpendicular to them.

The influence of "Rz" on the coat thickness on gray and nodular cast iron applied on silumin AlSi11 at t_k = 750°C and for the time τ = 180 s is presented in Figure 18.

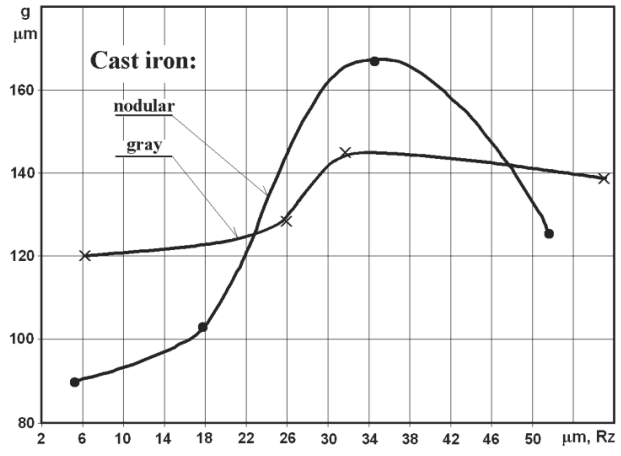

Fig. 18. The influence of "Rz" on the coat thickness on gray and nodular cast iron

It shows that regardless of the cast iron type, initially when the "Rz" grows, the thickness of the coat increases, especially intensively on nodular cast iron, up to a certain critical value; when this value is achieved it starts decreasing, very intensively for nodular cast iron. The critical values "Rz" and "Ra" for gray and nodular cast iron are respectively: Rz = 31.43 µm (Ra = 5. 55 µm) i Rz = 34.57 µm (Ra = 4.92 µm). The examples of the coat thickness on cast irons with different "Rz" are shown in Figure 19 (a-d) for gray cast iron and 20 (a-d) for nodular cast iron.

It follows from the presented data that the surface roughness "Rz" ("Ra") should be taken into consideration in the mechanism of coat formation. It is likely that a small roughness height "Rz" of the surface of the cast iron element, e.g. after finishing, results in a relatively small contact surface of the element with the bath. In connection to this, the object is heated in its complete volume to the temperature of the contact "t_s" in a relatively long time. The increase of "Rz" to the critical value causes the growth of the object's surface contact with the liquid metal bath. Fast heating of the tops takes place, and then of the whole roughness to the temperature "t_s". As a result, the intensiveness of heating of the specimen grows in the direction of the axis. Exceeding the critical value of "Rz" causes the increase in the surface field of the roughness tops and decreases the intensity of their heating, and thus of the whole cross section of the object. Again the time of the object heating to the temperature "t_s" gets longer. At the further stage, due to wetting of the specimen by liquid silumin and the viscosity processes the reactive diffusion of the Al and Si atoms takes place from the object to the bath side. Merging of the roughness takes place. At a small value of "Rz" after finishing, the difference of the concentration of Al, Fe and Si between the area where the roughness top was and the hollow is small. As a result, the concentration supercooling and the solid substance phase caused by the surface negative curvature of the division liquid - solid body are small and in connection to this the quickness of the phase $Al_{12}Fe_3Si_2$ grows and then $Al_9Fe_3Si_2$ and later silumin is small. The coat with the small thickness is being formed. The growth of "Rz" to the critical value due to fast heating of the roughness intensifies the reactive diffusion. Fast merging of the roughness takes place. Regarding the big height of the roughness, the difference of the concentration of the Al, Fe and Si between the hollow of a big radius and the area in which there was the roughness top is significant. In this area there appears considerable concentration supercooling, probably more considerable due to the negative curvature of the hollows. As a result supercooling in the hollow areas becomes bigger than in the areas of the merged roughness tops, which causes fast crystallization of a relatively thick layer of the phases $Al_{12}Fe_3Si_2$ and $Al_9Fe_3Si_2$. Exceeding the critical value of "Rz" causes the decrease in the intensity of heating of the roughness and the object to the temperature "t_s". As a result, cutting time of the given processes takes place. It is likely that the concentration supercooling also reduces, as well as the negative curvatures of the surface of the division liquid - solid body. It causes a decrease in the coat thickness.

Application of the Al-Si coat on the cast iron elements is mainly aimed at making the layered item cast iron - coat - silumin. A classical example of this item is a cast iron fitting embathed with cylinder silumin when casting heavy duty cylinders for combustion engines. In order to obtain the correct joining of the cylinder cast with the fitting, the Al-Si coat is applied, which makes joining with cylinder silumin possible during cylinder casting in a metal mould. The examples of joining gray and nodular cast iron via the Al-Si coat with silumin AlSi11 is shown in Figure 21 (a, b).

Figure 22 (a, b) show an example of a layered item consisting of gray cast iron - Al-Si coat - alloy AlSi1.5 (a) and gray cast iron - Al-Si coat - alloy AlSi17 (b).

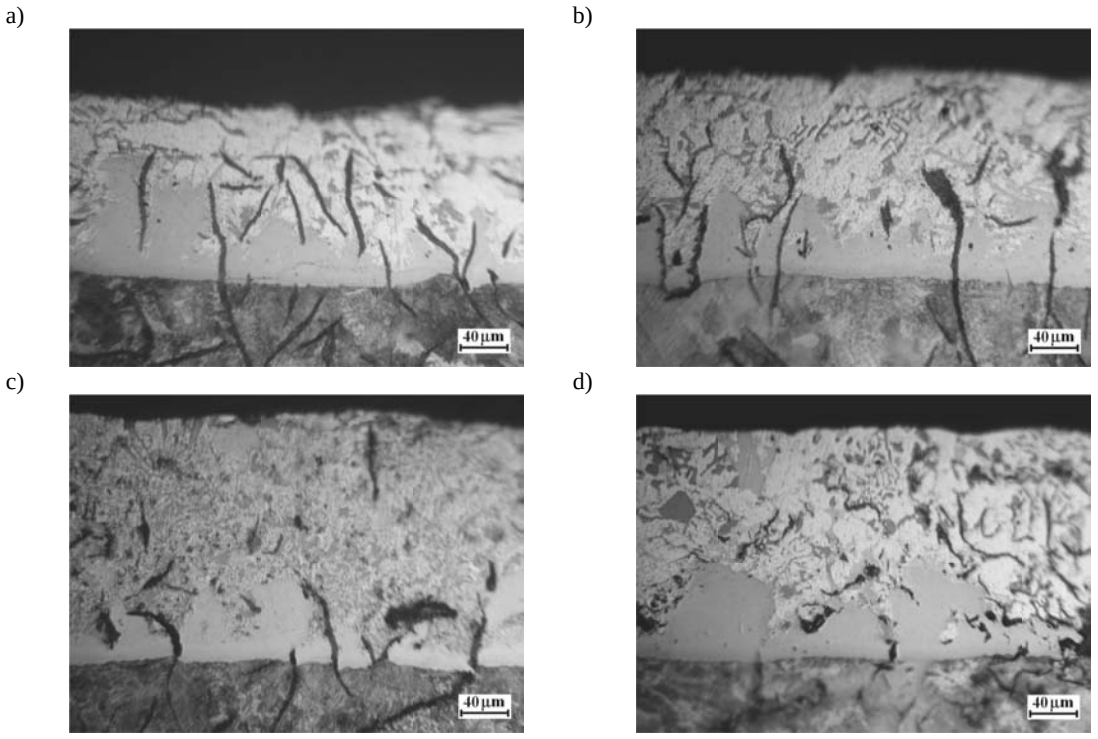

Fig. 19 (a-d). The representative coats obtained on the specimens made of gray cast iron with Rz(Ra): a - 6.40(0.95) µm; b - 25.90(3.46) µm; c - 31.43(5.55) µm; d - 56.97(10.46) µm

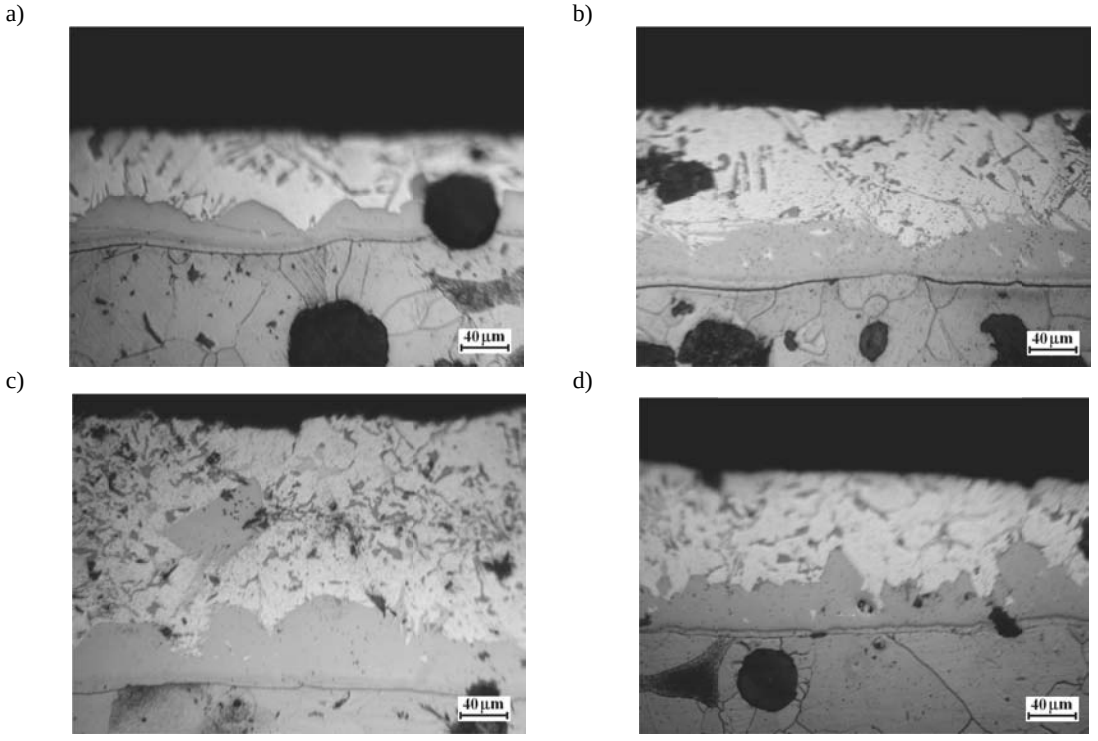

Fig. 20 (a-d). The representative coats obtained on the specimens made of nodular cast iron with Rz(Ra): a - 5.13(0.76) µm; b - 17.75(2.47) µm; c - 34.57(4.92) µm; d - 51.50(9.91) µm

a)

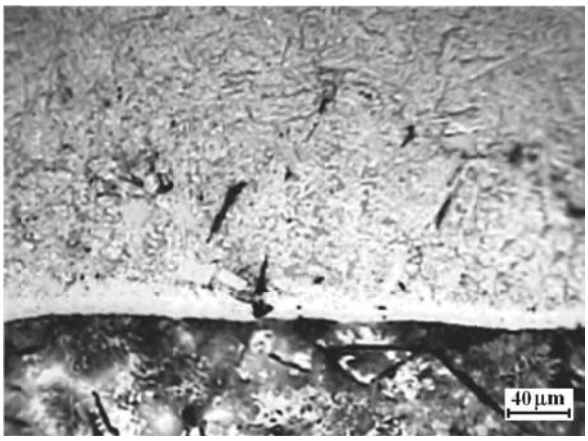

b)

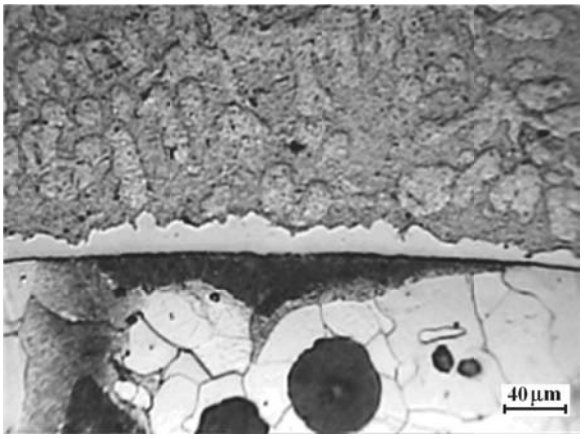

Fig. 21 (a, b). An example of joining of items made of gray (a) and nodular (b) cast iron via the Al-Si coat with silumin AlSi11

It is obvious that the thickness of the coat during making of the item decreases. The thickness of the layer in which there is a phase precipitation $Al_9Fe_3Si_2$ also decreases. It is caused by melting of the coat by silumin which is a part of the layered item. In the case of the layered item making from the non-alloy silumin Al-Si the phase structure of the joining is analogous to the coat structure.

In many cases silumin with such alloy additives as Ni, Mg and Cu is used on items, these additives increase their mechanical strength. The quantity of the alloy additives usually does not exceed 1.5 %. In this respect the coat structure and joining of silumins containing Ni, Mg and Cu were tested. The thickness of certain layers and the whole coat does not practically changes in relation to the earlier presented gray and spheroid cast iron.

An example of joining of the layered item via the coat applied in the AlSi11Cu1,5Ni1,5Mg0,5 bath with the same silumin on gray and nodular cast iron is shown in Figure 23 (a, b). It can be seen that the joining is highly hermetic and dense. Picture 24 shows the microstructure of the coat applied in the silumin AlSi11Cu1,5Ni1,5Mg0,5 bath on nodular cast iron, and Figure 25 presents the scheme of distribution of the following elements in this area: Al, Fe, Si, Cu, Mg and Ni.

a)

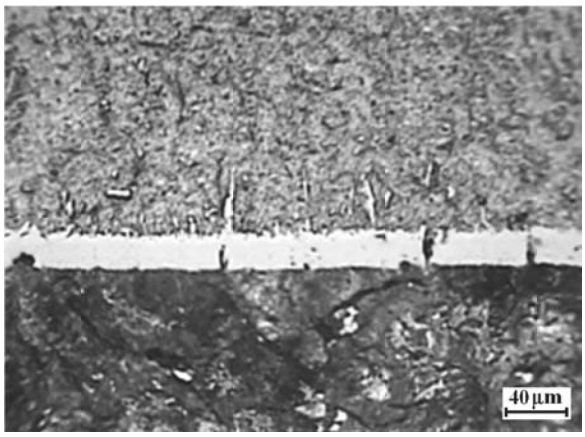

b)

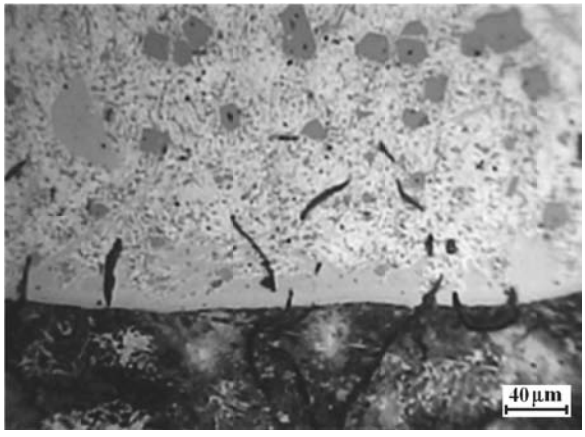

Fig. 22 (a, b). An example of a layered item in the system of gray cast iron - Al-Si coat - alloy AlSi1.5 (a) and gray cast iron - Al-Si coat - alloy AlSi17 (b)

They show that different intermetallic phases appear in the coat. These phases are analogous on nodular and gray cast iron. For example, points “1-4” in which the concentration of the elements was tested in the coat poured with silumin AlSi11Cu1.5Ni1.5Mg0.5 on gray cast iron is shown in Figure 26 (a, b)

The concentration of the elements tested in the area marked as No “1” is presented in Table 11.

Table 11.
The concentration of the elements tested in the area marked as No “1”

Element	k-ratio (calc.)	ZAF	Atom %	Element Wt %	Wt % Err. (1-Sigma)
Al-K	0.1041	1.748	29.75	18.19	+/- 0.13
Si-K	0.0453	1.590	11.32	7.21	+/- 0.07
Mg-K	0.0000	2.375	0.00	0.00	+/- 0.00
Fe-K	0.7138	1.043	58.82	74.46	+/- 0.62
Ni-K	0.0013	1.088	0.11	0.14	+/- 0.18
Cu-K	0.0000	1.120	0.00	0.00	+/- 0.00
Total			100.00	100.00	

a)

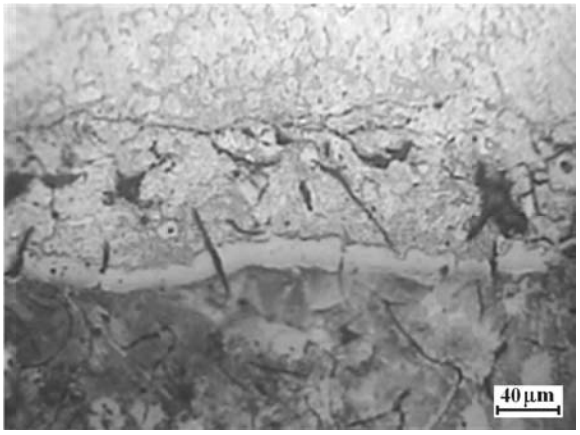

b)

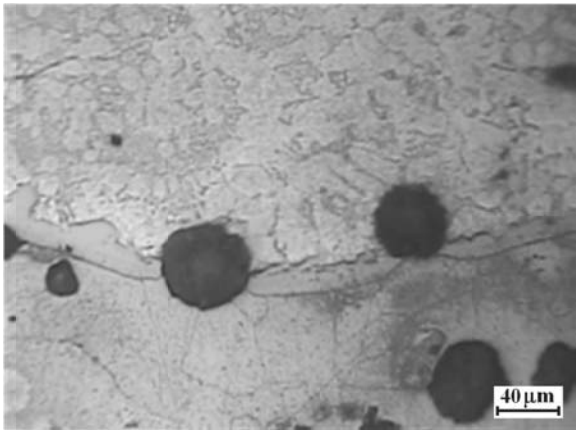

Fig. 23 (a, b). An example of joining of silumin AlSi11Cu1.5Ni1.5Mg0.5 via the coat with gray (a) and nodular (b) cast iron

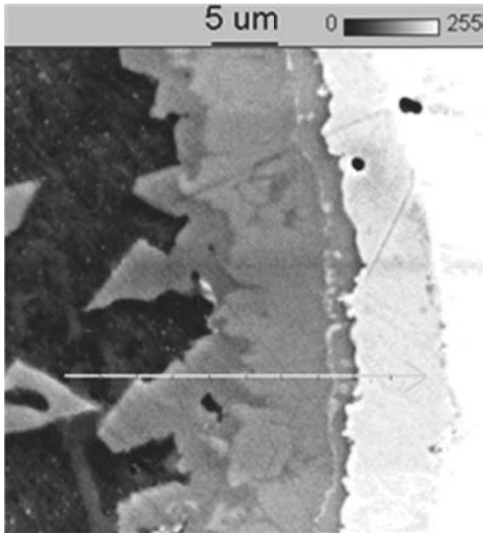

Fig. 24. The microstructure of the coat applied in the bath AlSi11Cu1,5Ni1,5Mg0,5 on nodular cast iron

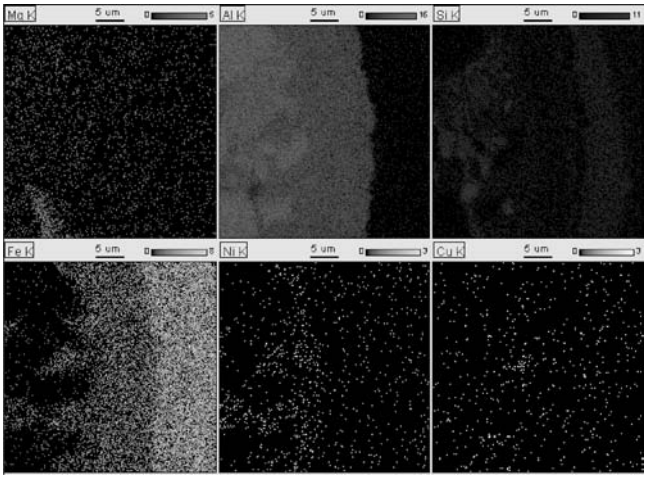

Fig. 25. The scheme of distribution of the elements in the area presented in Fig. 24

a)

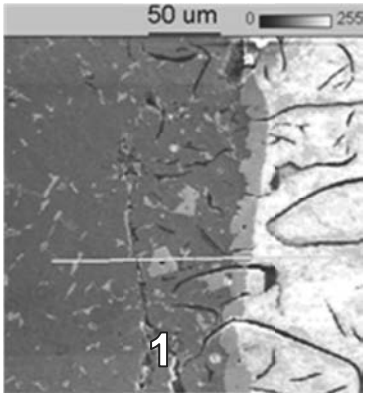

b)

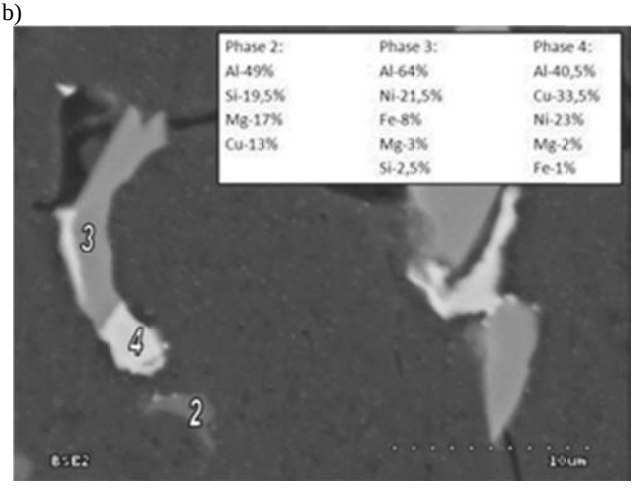

Fig. 26 (a, b). The location of points 1-4 in which the test to check the concentration of Al, Si, Mg, Fe, Cu and Ni was performed in the layered cast consisted of gray cast iron - coat applied in AlSi11Cu1,5Ni1,5Mg0,5 - silumin analogous to the one applied on the coat

It follows from the presented data that phase $Al_9Fe_3Si_2$ is marked as No "1", phase AlSiMgCu - as No "2", phase $Al_3NiFeMgSi$ - as No "3" and phase AlCuNi - as phase No 4. In this connection it can be stated that in the layered joining the intermetallic phases crystallize containing the alloy additives present in silumin. The inter-phase border of $Al_3NiFeMgSi$/liquid silumin is the base for crystallization of the phase AlCuNi. A similar structure of joining appears on nodular cast iron as well. As it was previously stated, during the coat formation on nodular cast iron, the first layer on it is carbide Fe_4CSi. It cannot be eliminated in the process of the layered cast making, which is proved by the tests the results of which are presented in Figure 27 (a, b).

It shows that the layer of carbide Fe_4CSi on nodular cast iron base is continuous, dense and hermetically adjusted to the base. Its chemical composition is very similar to the one presented in Table 8.

a)

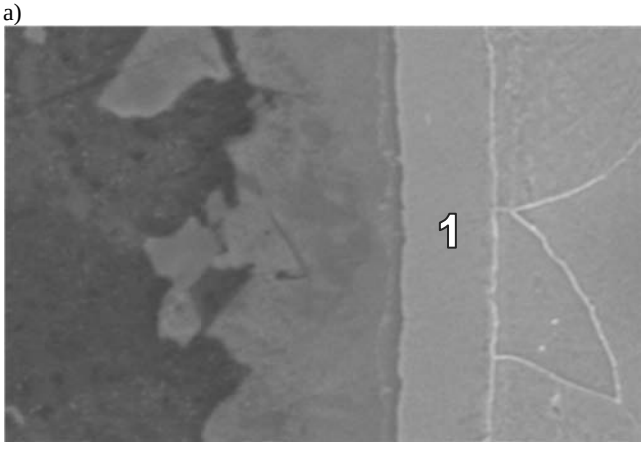

b)

Element	k-ratio (calc.)	ZAF	Atom %	Element Wt %	Wt % Err. (1-Sigma)
C -K	0.0132	4.501	20.62	5.95	+/- 0.14
Al-K	0.0035	1.872	1.02	0.66	+/- 0.07
Si-K	0.0808	1.472	17.63	11.90	+/- 0.10
Fe-K	0.7799	1.045	60.73	81.49	+/- 0.62
Total			100.00	100.00	

Fig. 27 (a, b). Layered cast nodular cast iron - silumin AlSi11Cu1,5Ni1,5Mg0 with the layer (marked as No "1") of carbide on cast iron (a) and its chemical composition (b)

Reassuming the presented research results it should be stated that joining between the cast iron element and the silumin via the silumin coat takes place as a result of silumin melting in the coat and partial melting and melting of the layer $Al_9Fe_3Si_2$. During the process of pouring of the layered cast, as a result of the turbulent and convectional movement of liquid silumin, a partial separation of the melted tops of the phase $Al_9Fe_3Si_2$ takes place and they were taken in the depth of silumin of the joining. In connection with it, its number and value increase in the area of joining. In alloy silumins the coat is built from a very complex phase AlFeSiCuNiMg. On nodular cast iron it is preceded by silicon carbide Fe_4CSi. Turbulent and convectional movement of the liquid metal, reaction diffusion and fast crystallization in the joining area of the cast iron element with the silumin via the coat cause appearance of nonequilibrium multi-component phases, such as: AlSiMgCu, Al_3NiFe, $Al_3NiCuFe$, $Al_3NiFeMgSi$, AlCuNi and $Al_9Fe_3Si_2$.

Application of the coat in over-eutectic silumin, e.g. AlSi14Cu1,5Ni1,5Mg0,5, causes appearance of a similar coat as in under-eutectic silumins. The structure of the joining of cast iron with silumin is also analogous to under-eutectic silumins. However, the phenomenon of the increase in the silicon concentration in the phases containing the silicon is observed.

On the bases of the presented results of the basic tests a technology of layered items making was worked out, it was tested positively in the industrial conditions. For instance, the layered item of the compressor body for room air-conditioning is presented below. The linear bushings of the compressor were made of low-alloy gray cast iron which via the silumin coat applied in the silumin bath AlSi9Cu1,5Ni1,5Mg0,5 was joined with the same silumin. The body of the compressor from the above mentioned silumin was cast in the mould. The cross-section of the layered body of the compressor is shown in Figure 28.

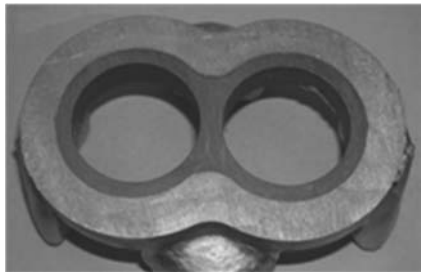

Fig. 28. The cross-section of the layered body of the compressor

As it can be seen, there is a very good joining of the silumin body with the cast iron linear bushings of the compressor.

The example of the silumin coat on a single linear bushing of the compressor applied in the industrial conditions is presented in Figure 29.

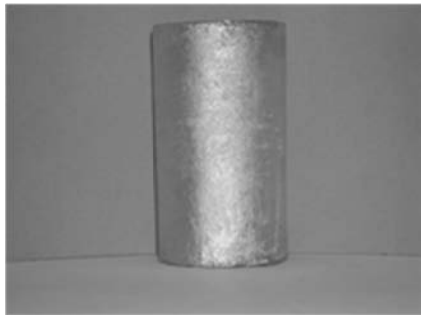

Fig. 29. The silumin coat on the cast iron linear bushing dipped into the bath AlSi9Cu1,5Ni1,5Mg0,5 in the industrial conditions.

The microstructure of the layered body of the compressor is shown in Figure 30.

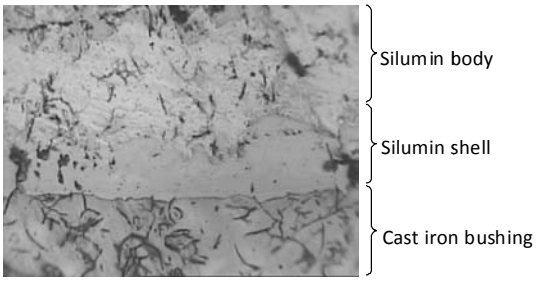

Fig. 30. The microstructure of the joining of the layered body of the compressor

On the bases of the results of the tests presented in this work, it can be stated that production of layered items will make it possible to decrease the weight of different constructive element. It is also possible to decrease the production costs and increase the quality and aesthetic of the items.

3. Summary

Reassuming the presented research results, the mechanism of the coat crystallization on cast iron can be presented as follows. The cast iron element preheated to the temperature of the initial heating is dipped in the Al-Si bath, alloy additives such as: nickel, magnesium and copper are also possible. The silicon concentration in the bath depends on the required thickness of the coat. Then at a certain time a local decrease in the bath temperature around the dipped element takes place and silumin crystallizes on it. At the same time the successive heating of the object takes place. The carried out simulation showed that silumin sets solid on the surface of the element and then melts again within the time of 0.1-0.2 s. Then heating of the element to the temperature of the contact "t_s" takes place. From now on, simultaneous heating of the upper layer of the object and the neighbouring silumin bath takes place due to the transfer of heat from the farther areas of the bath and its convectional movements. It is likely that then the process of surface merging of the cast iron object by the aluminum begins. The intensity of the surface merging is very high. Reactive diffusion of the iron and silicon atoms, and possibly of the alloy additives (Ni, Cu, Mg) as well, starts from the bath to the surface of the element and their absorption. At the surface of the element the concentration of Fe, Al and Si increases. There appears the liquid alloy Al-Fe-Si which contains the phase Al_3Fe at first which is supercooled regarding the peritectic temperature, as a result of which a peritectic reaction takes place: $L+Al_{12}Fe_3Si_2 \rightarrow L+Al_9Fe_3Si_2$. The phase $Al_9Fe_3Si_2$ grows on the phase $Al_{12}Fe_3Si_2$ which party merges.

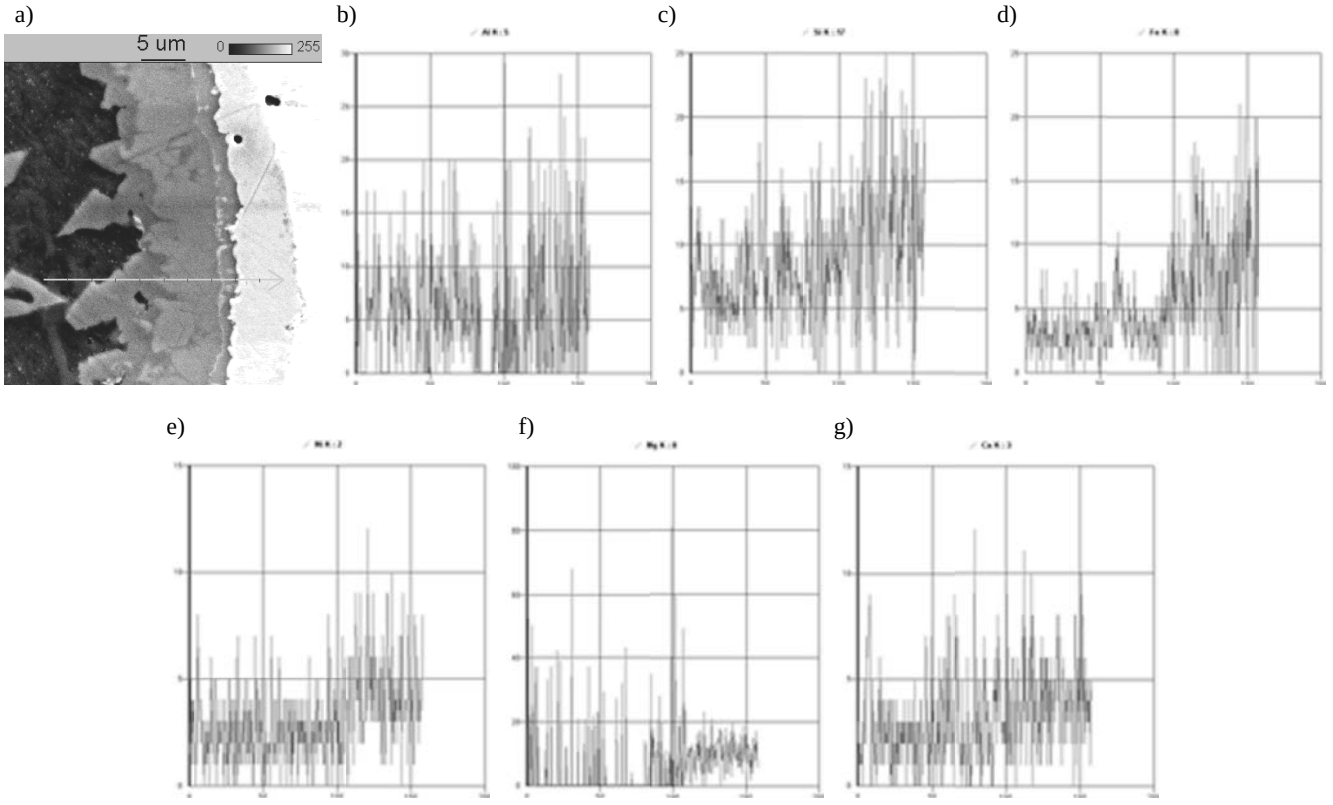

Fig. 31 (a-g). The microstructure of the coat applied in silumin AlSi11Cu1,5Ni1,5Mg0,5 at t_k = 750 and τ = 180 s (a) with the measuring line and linear distribution of the composing elements of silumin (b-g)

In nodular cast iron, in the first period iron-silicon carbide Fe_4CSi crystallizes immediately on the object's surface. It is possibly caused by the fact that flaked graphite appears in gray cast iron, thus the quantity of pearlite merged by the aluminum is small; so the quantity of the carbon from the merged cement carbide in the bath surrounding the surface of the object is not enough to form carbide Fe_4CSi. In nodular cast iron taking into account spherical precipitations of graphite the quantity of cement carbide merged by aluminum is significantly bigger, which causes high saturation of the bath by carbon and thus carbide Fe_4CSi crystallizes first of the base, and then peritectically the phases $Al_{12}Fe_3Si_2$ and $Al_9Fe_3Si_2$. In the process of the coat crystallization the height of the roughness "Rz" of the object's surface covered by the coat is also important and was previously presented.

The coats on the iron casts applied in silumins with alloy additives: Ni, Mg and Cu are different in terms of their chase structure from the ones applied in the Al-Si bath. Figure 31 (a-g) shows the microstructure of the coat with the measuring line on nodular cast iron applied in silumin AlSi11Cu1,5Ni1,5Mg0,5 (a) and linear distribution of: Al, Si, Fe, Ni, Mg and Cu (b-g).

The point analysis of certain phases is also presented. It was stated that the first phase crystallizing of the element is a complex phase AlSiFeCuNiMg. The $Al_3NiFeMgSi$ phase crystallizes on it first and then the phase AlNiFeSi. Apart from these phases there are phases of silumin Al, eutectic Al+Si and the phases $Al_9Fe_3Si_2$, $Al_3NiFeCu$, $AlNiCu$, Al_3NiCu.

It follows from the presented data that the process of the coat crystallization and the structure which follows from it are very complex. In the layered joining the phases remain the same, though the thickness of the coat in the area of silumin changes.

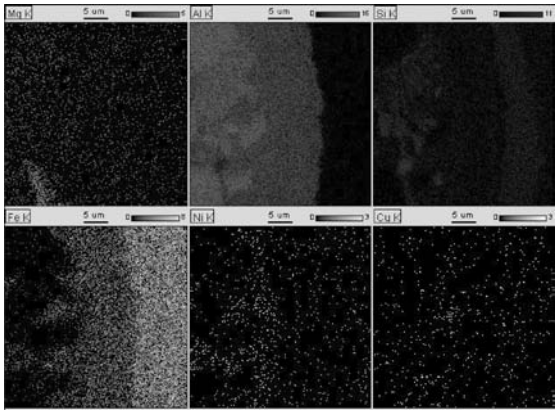

Fig. 32. The scheme of distribution of: Al, Fe, Si, Cu, Mg and Ni in the area presented in Fig. 31 a

On the basis of the data presented in the whole work it should be stated that the process of the Al-Si coat application, possibly with the alloy additives such as: Ni, Mg and Cu, on gray and nodular cast iron is very complex. In the area at the surface of the element there is an intensive convectional movement of the metal bath causing the transfer of some crystals of the phases $Al_9Fe_3Si_2$ or AlSiFeCuNiMg into the depth of the liquid silumin. The process of the coat or the joining crystallization happens very fast within the time not more than 180 s and 300 s respectively.

Generally it is necessary to state that in order to work out the correct production technology of application of the coat and possibly making layered items from aluminum alloys with silicon or other alloy additives, it is necessary to take into consideration the theoretical basis of crystallization and the phase structure of the coat presented in this work as well as the factors which influence them.

The scheme of the concentration of: Al, Fe, Si, Cu, Mg and Ni in the area is presented in Figure 31 a is shown in Figure 32.

Acknowledgements

Scientific work financed from the funds for science in the years 2009-2012 as research Project No N N508 4378 36

References

[1] S. Pietrowski, Crystallization, structure and properties of the piston silumins, Publisher Technical University of Łódź, 1999 (in Polish).
[2] J.C. Viala, M. Peronnet, F. Barbeau, F. Bosselet, J. Bouix, Interface chemistry in aluminum alloy casting reinforced with iron base inserts, Composites A 33 (2002) 1417-1420.
[3] T. Szymczak, Model of coat increase on iron alloys hot dip obtained in Al-Si bath and its connection with multicomponent silumins, PhD Thesis, Technical University of Łódź, 2007 (in Polish).
[4] S. Pietrowski, T. Szymczak, The structure of connection of alphinizing coat with silumin, Archives of Foundry 14 (2004) 20-30 (in Polish).
[5] K. Żaba, S. Nowak, S. Kąc, S. Starzykowski, Analysis of tool wear in the perforation process of steel strips coated Al-Si, for the elements of exhaust systems, Ores and Metals 2 (2006) 71-78 (in Polish).
[6] A. Gierek, L. Bajka, Dip aluminized - properties and application, Design Issues 12 (1976) 356-360 (in Polish).
[7] S. Pietrowski: Structure of alfinizing layer on the gray cast iron, Archives of Foundry 11 (2004) 33-38 (in Polish).
[8] S. Pietrowski, T. Szymczak, The structure of Al-Si immersing coatings on iron alloys, Archives of Foundry 12 (2004) 7-16 (in Polish).
[9] S. Pietrowski, L. Klimek, T. Szymczak, Diffraction research of the alphinizing coat on iron alloys, Archives of Foundry 22 (2006) 22-28 (in Polish).
[10] S. Pietrowski, T. Szymczak, The structure of the alphinizing coat on alloy steels, Archives of Foundry Engineering 8/4 (2008) 229-235.
[11] S. Pietrowski, T. Szymczak, Alfinated coating structure on HS6-5-2 (SW7M) high speed steel, Archives of Foundry Engineering 10/4 (2010).
[12] T. Szymczak, The structure of connection of the AlSi5 - HS6-5-2 compound casting obtained by alphinising, Archives of Foundry Engineering 11/ 3 (2011).
[13] J. Taler, P. Duda, Solving simple and inverse heat conduction problems, WNT, Warsaw, 2003 (in Polish).
[14] S. Pietrowski, Silumins, Publisher Technical University of Łódź, 2001 (in Polish).
[15] K. Sękowski, J. Piaskowski, Z. Wojtowicz, Atlas of standard alloys structures, WNT, Warsaw, 1972 (in Polish).
[16] C. Podrzucki, Cast iron, The structure, properties, applications, ZG STOP, Cracow, 1991 (in Polish).